The Journal of Organic Chemistry

Subscriber access provided by BUFFALO STATE

Article

Reactions of Thiiranium and Sulphonium ions with Alkenes in the Gas-phase

Samuel Charles Brydon, Shea Fern Lim, George N. Khairallah, Philippe Maitre, Estelle Loire, Gabriel da Silva, Richard A. J. O'Hair, and Jonathan M White

J. Org. Chem., **Just Accepted Manuscript** • DOI: 10.1021/acs.joc.9b01264 • Publication Date (Web): 22 Jul 2019

Downloaded from pubs.acs.org on July 23, 2019

Just Accepted

"Just Accepted" manuscripts have been peer-reviewed and accepted for publication. They are posted online prior to technical editing, formatting for publication and author proofing. The American Chemical Society provides "Just Accepted" as a service to the research community to expedite the dissemination of scientific material as soon as possible after acceptance. "Just Accepted" manuscripts appear in full in PDF format accompanied by an HTML abstract. "Just Accepted" manuscripts have been fully peer reviewed, but should not be considered the official version of record. They are citable by the Digital Object Identifier (DOI®). "Just Accepted" is an optional service offered to authors. Therefore, the "Just Accepted" Web site may not include all articles that will be published in the journal. After a manuscript is technically edited and formatted, it will be removed from the "Just Accepted" Web site and published as an ASAP article. Note that technical editing may introduce minor changes to the manuscript text and/or graphics which could affect content, and all legal disclaimers and ethical guidelines that apply to the journal pertain. ACS cannot be held responsible for errors or consequences arising from the use of information contained in these "Just Accepted" manuscripts.

is published by the American Chemical Society. 1155 Sixteenth Street N.W., Washington, DC 20036

Published by American Chemical Society. Copyright © American Chemical Society. However, no copyright claim is made to original U.S. Government works, or works produced by employees of any Commonwealth realm Crown government in the course of their duties.

Reactions of Thiiranium and Sulphonium Ions with Alkenes in the Gas-Phase

Samuel C. Brydon[a], S. Fern Lim[a], George N. Khairallah[a,b], Philippe Maître[c], Estelle Loire[c], Gabriel da Silva[d], Richard A. J. O'Hair[a], Jonathan M. White[a*]

[a] *School of Chemistry and Bio21 Institute, The University of Melbourne, Parkville, Victoria 3010, Australia.*

[b] *Accurate Mass Scientific Pty Ltd, P.O. Box 92, Keilor VIC 3036, Australia*

[c] *Laboratoire de Chimie Physique (UMR8000), Université Paris-Sud, CNRS, Université Paris Saclay, Orsay, 91405, France*

[d] *Chemical and Biomolecular Engineering, University of Melbourne, Parkville, Victoria 3010, Australia.*

Email:

whitejm@unimelb.edu.au

Abstract:

Ion-molecule reactions between thiiranium ion **11** (*m/z* 213) and cyclohexene and *cis*-cyclooctene resulted in the formation of addition products **17a** and **17b** (*m/z* 295 and *m/z* 323 respectively) *via* an electrophilic addition pathway. Associative π-ligand exchange involving direct transfer of the PhS^+ moiety, which has been observed for analogous seleniranium ions in the gas-phase, did not occur despite previous solution experiments suggesting it as a valid pathway. DFT calculations at the M06-2X/def2-TZVP level of theory showed high barriers for the exchange reaction, whilst the addition pathway was more plausible. Further support for this pathway was provided with Hammett plots showing the rate of reactivity to increase as the benzylic position of thiiranium ion derivatives became more electrophilic ($\rho = +1.69$; $R^2 = 0.974$). The more reactive isomeric sulphonium ion **22** was discounted as being responsible for the observed reactivity with infrared spectroscopy and DFT calculations suggesting little possibility for isomerisation. To further explore the differences in reactivity, thiiranium ion **25** and sulphonium ion **27** were formed independently with the latter ion reacting over 260 times faster towards *cis*-cyclooctene than the thiiranium ion rationalised by calculations suggesting a barrierless pathway for sulphonium ion **27** to react with the cycloalkene.

Introduction:

Thiiranium ions (general structure **1**, **Scheme 1**) have been shown to be important reactive intermediates in many synthetic transformations, particularly in the stereoselective functionalisation of alkenes.[1-16] These intermediates are typically formed by either addition of an electrophilic chalcogen reagent to an alkene (**Path A, Scheme 1**) or by the chalcogen lone-pair induced elimination of a suitable β-leaving group, such as an alcohol following acid treatment or halides in the presence of silver salts (**Path B, Scheme 1**).[1,3,4,6] Though readily available reagents such as phenylsulphenyl chloride can be used as an electrophilic sulphur source, more complex species such as trisulphur salts have become popular as they allow stereoselectivity induction at the sulphur source itself rather than at the alkene.[3,8,9,11,17]

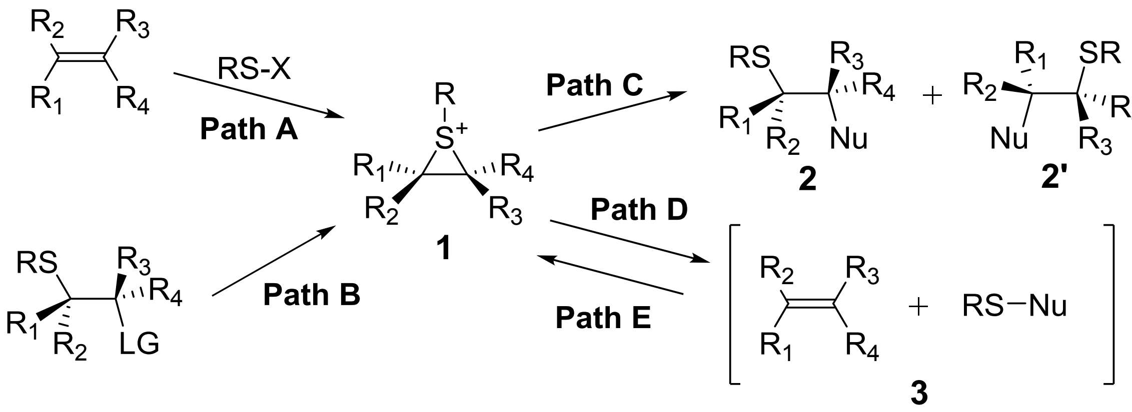

Scheme 1. Possible pathways for formation and reaction of thiiranium ion **1**

Rather than undergoing reactions as conventional *n*-type reactive intermediates, thiiranium ions follow two pathways. The first involves nucleophilic attack at the α-carbon yielding products **2** and **2’** (internal nucleophiles give cyclised products), which are themselves useful synthetic building blocks as stereochemical integrity is maintained due to anchimeric assistance by the chalcogen atom (**Path C, Scheme 1**).[1,2,4,18-22] The alternative is nucleophilic attack at the chalcogen centre (**Path D, Scheme 1**) to give an alkene and a highly electrophilic sulphur transfer agent **3**, which may further undergo π-ligand exchange.[5,8,23-26] This reversible process contributes to the limitations of some chalcogen iranium ions in synthesis, particularly for the more electrophilic selenium, as stereochemistry of these species is scrambled.[5,7,8,24] Investigations into the effects of varying the R group directly on the chalcogen of both thiiranium and seleniranium ions in solution have shown that more bulky groups tend to maintain optical purity, whilst both electron donating and withdrawing groups had minimal impact on the stereo outcome for sulphur substrates.[8,10,27,28] However, electron donating groups such as p-OMe-phenyl on the selenium of the iranium ion intermediate lead to extensive scrambling compared to electron withdrawing groups such as o-NO$_2$-phenyl, which maintained stereochemical integrity, a result which was rationalised by the latter activating the α-carbon of the iranium ion toward nucleophilic attack.[29-31]

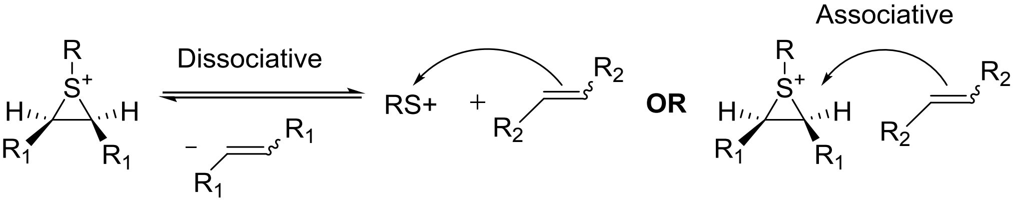

Scheme 2. Dissociative and associative transfer mechanisms of RS^+ between alkenes

The formal olefin-to-olefin RS^+ transfer has previously been thought to be dissociative and involve nucleophilic assistance with formation of the electrophilic transfer reagent in **3** (RS-Nu, **Scheme 1**). However, Denmark *et al.* have reported transfer of the RS^+ moiety (R = Ph only; R = Me showed no transfer) between olefins to be associative by generating thiiranium ions in the presence of the relatively non-nucleophilic counterion SbF_6^- in a non-participating solvent, CD_2Cl_2 (**Scheme 2**).[5,24]

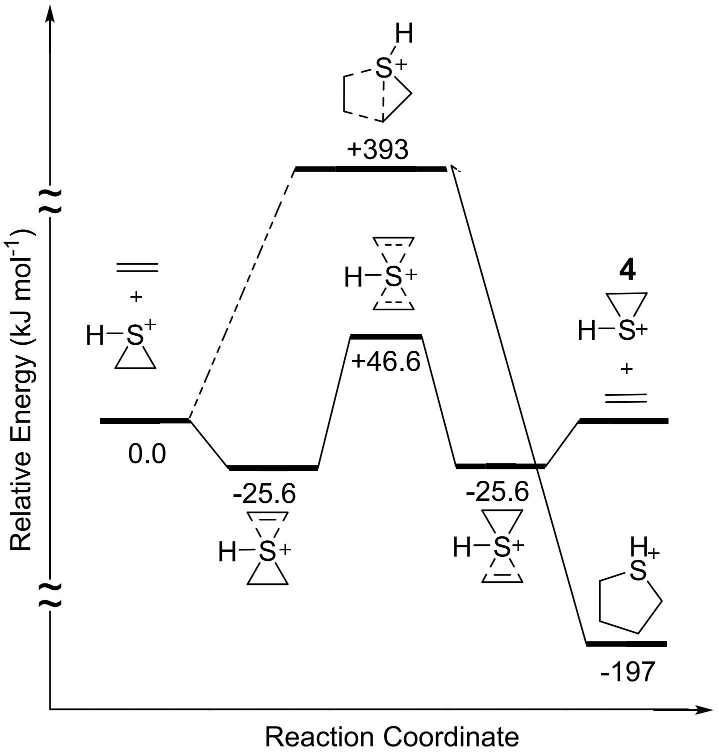

Figure 1. Relative energy diagram for reaction pathways of ethene with thiiranium **4**. Calculated at G2 (ZPVE = MP2) level of theory. Electronic energies reported at 0 K in kJ mol^{-1} with scaled ZPVE. Adapted from Reference 25.

Though this process was slow even at the higher temperature of 0°C (no transfer was observed at -20°C), the higher temperatures reflected theoretical calculations by Radom suggesting that direct transfer of the RS^+ group was feasible between ethene molecules with a kinetic barrier of 46.6 kJ mol^{-1} compared to a thermodynamically preferable insertion product (-197 kJ mol^{-1}) that required a much higher barrier of 393 kJ mol^{-1} (**Figure 1**).[25]

Mass spectrometry has grown to be a powerful technique for investigating the reactivity of charged species in the gas-phase.[32-35] This technique removes complications from solvents, counterions and potential impurities allowing for more accurate insights into reaction mechanisms, such as differentiating associative *vs* dissociative π-ligand exchange reactions of chalcogen iranium ions (**Scheme 2**). In combination with theoretical calculations, multi-stage mass spectrometry experiments have been used to probe the olefin-to-olefin RSe^+ transfer in the gas-phase.[36]

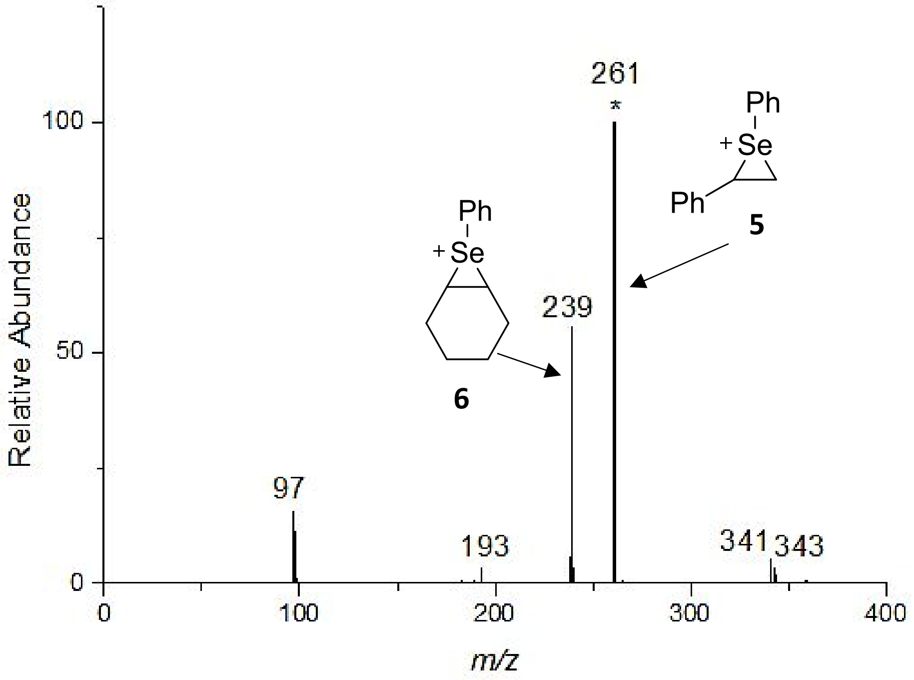

Figure 2. Ion-molecule reaction between seleniranium ion **5** *m*/z 261 and cyclohexene (at a concentration of *ca* 10^{11} molecules cm^{-3} for $t = 25{,}000$ ms). The mass selected ion is denoted by an asterisk (the most abundant selenium isotope ^{80}Se was used). Adapted from Reference 36.

The observed seleniranium ion **5** structure was confirmed through a combination of high-resolution mass spectrometry (HRMS), infra-red multiple photon dissociation spectroscopy (IRMPD), ion-mobility measurements, and DFT calculations.[36] Once mass selected, seleniranium ion **5** was shown to undergo π-ligand exchange *via* an associative mechanism in ion-molecule reactions (IMR) with a variety of cycloalkenes, with increasing rates of reactivity corresponding to an increase in ring strain of the cycloalkene.[37-39] For example, upon exposure to cyclohexene introduced directly into the spectrometer, there was a loss of parent seleniranium ion intensity *m/z* 261 and the formation of an ion at *m/z* 239 **6** reflecting the direct transfer of the $PhSe^+$ moiety from styrene to cyclohexene *via* a thermodynamically driven pathway supported by DFT calculations (**Figure 2**). The transition states for π-ligand exchange reactions also appear to bear the hallmarks of coarctate transition states with concomitant bond formation and breakage occurring at the central chalcogen, but this requires further investigation.[40]

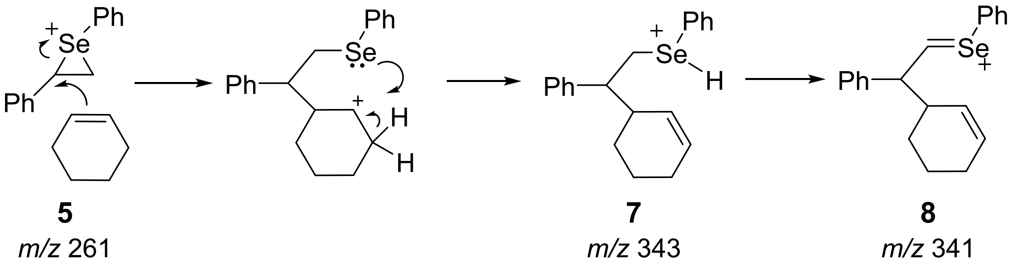

Scheme 3. Proposed mechanism for formation of addition/elimination product ions **7** and **8**

The appearance of an accompanying smaller peak at *m/z* 343 was assigned to an electrophilic addition product **7** following proton transfer from the initial adduct. Apparent 'spontaneous elimination' of H_2 could plausibly give the product **8** corresponding to the observed peak at *m/z* 341. However, this was later shown to be an artefact of a highly reactive impurity in the aged cycloalkenes, possibly a result of auto-oxidation. The other side-products were attributed to oxidation of the alkene *via* initial hydride transfer to the electrophilic iranium ion followed by reactions with water and neutral alkene.[36]

Though Denmark's solution experiments showed very high reactivity for seleniranium ions, the results indicated relatively slow π-ligand exchange for the corresponding thiiranium ions and in some cases no reaction was observed.[24] Given the gas-phase results for the reactivity of seleniranium ions towards cycloalkenes, particularly the support for an associative π-ligand exchange mechanism, we believed it would be interesting to investigate the reactivity of thiiranium ions with alkenes under similar conditions.

Results and Discussion:

Various sulphur substrates were used to generate a range of thiiranium ions allowing for a greater scope of investigation than the previously explored seleniranium ions. One such variation was the leaving group with an acetate group employed rather than an amine, allowing for easier syntheses of appropriate thiiranium ion precursors. The β-thiophenylacetate **9** was introduced as a single regioisomer at a concentration *ca* 0.1 mM in acetonitrile with 1% formic acid into the mass spectrometer under electrospray ionisation (ESI) conditions (**Scheme 4**).

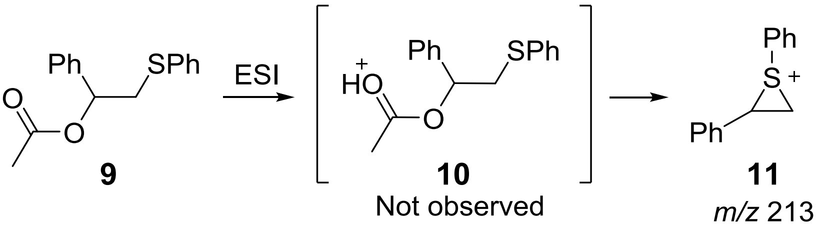

Scheme 4. ESI of acetate precursor **9** to give thiiranium ion **11** (*m/z* 213)

Unlike the previously studied β-selenylamines, which gave an ammonium ion upon ESI, the β-thiophenylacetate **9** did not produce an observable protonated ion, but rather directly produced **11** in the ESI source (**Scheme 4**).[36] Extensive investigations were undertaken previously with selenium to provide evidence for the structure of the ion at *m/z* 261 to be that of the seleniranium ion **5** as discussed. It was reasonable to assume at this stage that the observed sulphur containing ion at *m/z* 213 generated under similar conditions would indeed be that of the corresponding thiiranium ion with HRMS supporting this assumption (see Supporting Information p S3). The ion **11** in all cases could then be further isolated (MS^2) and allowed to undergo ion-molecule reactions with a variety of volatile alkenes. Initial investigations into the gas-phase bimolecular reactivity of thiiranium ion **11** involved conducting IMR with cyclohexene and *cis*-cyclooctene in the ion-trap of the mass spectrometer as with the previous studies for seleniranium ion **5**. Following isolation, thiiranium ion **11** (*m/z* 213), produced via ESI of acetate precursor **9**, was independently exposed to a stream of cyclohexene and *cis*-cyclooctene introduced at concentrations of *ca.* 2-3 x 10^{11} and 6-7 x 10^{10} molecules cm^{-3} respectively.

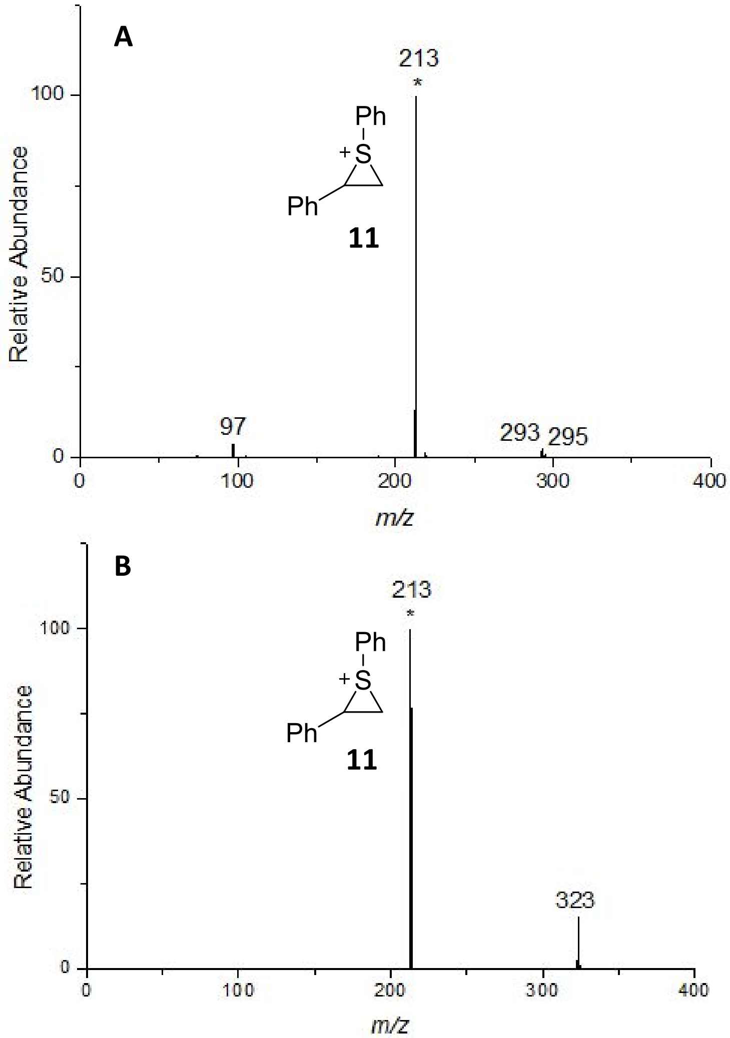

Figure 3. IMR of thiiranium ion **11** *m/z* 213 with **A)** cyclohexene (t = 8000 ms) and **B)** *cis*-cyclooctene (t = 8000 ms) at a concentration of *ca* 10^{11} molecules cm^{-3}. The mass selected ion is denoted by an asterisk (the most abundant sulphur isotope ^{32}S was used in all experiments).

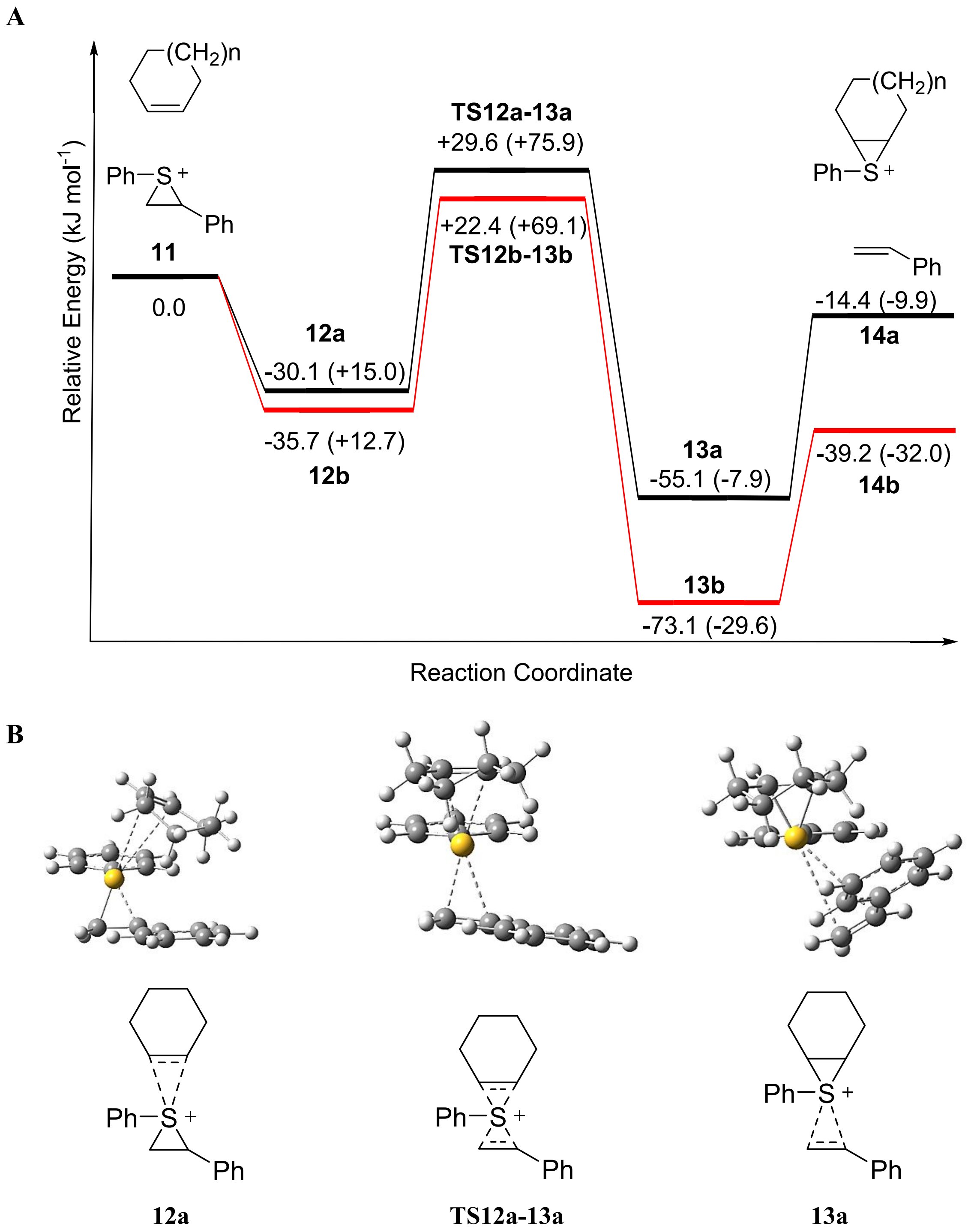

Figure 4. **A)** Relative energy diagram for π-ligand exchange of cyclohexene (a: n = 1, black) and *cis*-cyclooctene (b: n = 3, red) with styrene at the sulphur of thiiranium ion **11**. Energies given as ΔH (ΔG) in kJ mol^{-1} at M06-2X/def2-TZVP level of theory relative to the total free reactant energies. **B)** Gaussview optimised structures of key species **12a**, **TS12a-13a** and **13a** with accompanying Chemdraw diagrams. (Refer to Supporting Information for *cis*-cyclooctene Gaussview structures).

Unexpectedly, no π-ligand exchange product (cyclohexene: *m/z* 191; *cis*-cyclooctene: *m/z* 219), which would be the result of an associative transfer mechanism, was observed during either of these reactions (**Figure 3**). Instead, the reactivity between the alkene and the thiiranium ion consisted of an addition pathway (cyclohexene: *m/z* 295; *cis*-cyclooctene: *m/z* 323),[41] previously observed with the seleniranium ions as a minor pathway.[36] Upon further investigation with DFT calculations, however, this result was less surprising with an enthalpic barrier of approximately +22 and +30 kJ mol^{-1} to associative π-ligand exchange for *cis*-cyclooctene and cyclohexene respectively (**TS12a-13a** and **TS12b-13b**, **Figure 4**). Note that unlike solution-phase, calculations predict the reaction will happen in the gas-phase when all species leading towards the product(s) are less than the enthalpy of the free reactants ($\Delta H < 0$), as there is no solvent present to provide additional energy to overcome endothermic barriers.[42] In addition, Dau *et al* have highlighted that the relevant thermodynamic parameter to use for low-pressure bimolecular reactions in the gas-phase is the reaction energy/enthalpy rather than the Gibbs free energy since the computed entropy of the reactants is not a good measure of the entropy at the entrance channel.[43] The high $\Delta G^{\ddagger}$ of the transition state (cyclohexene: +76 kJ mol^{-1} ; *cis*-cyclooctene: +70 kJ mol^{-1}) relative to the reactants indicates that there is an additional entropic barrier to this reaction occurring in the gas-phase, most likely a result of the tightly restricted orientation of the alkenes at the chalcogen during the transition state (**Figure 4**). Combined, the enthalpic and entropic barriers prevent associative π-ligand exchange occurring for thiiranium ion **11** under these conditions.

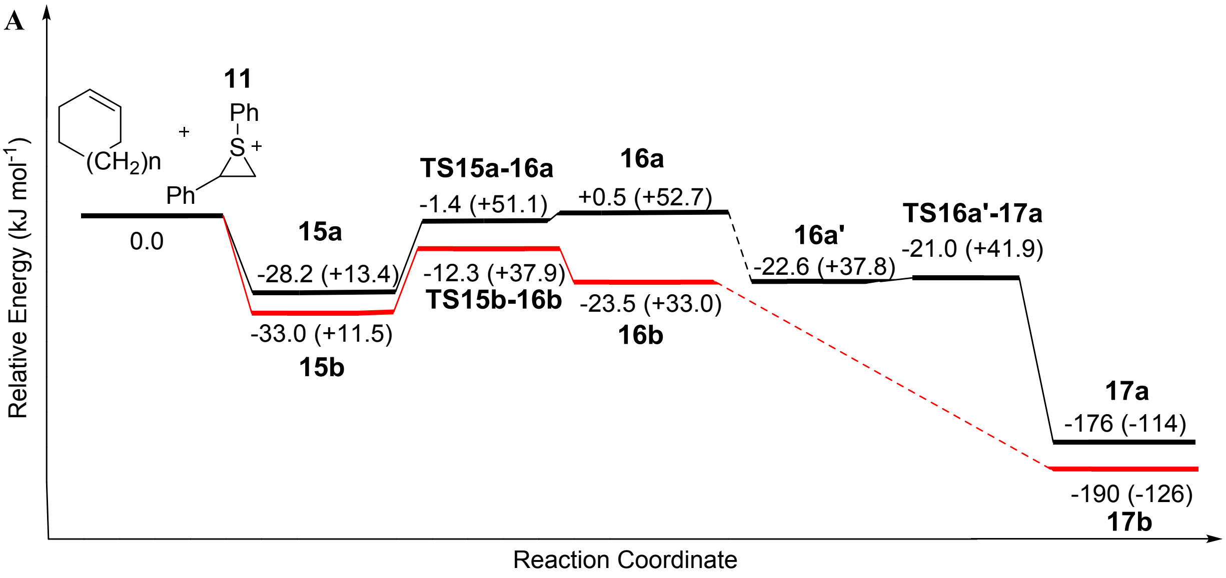

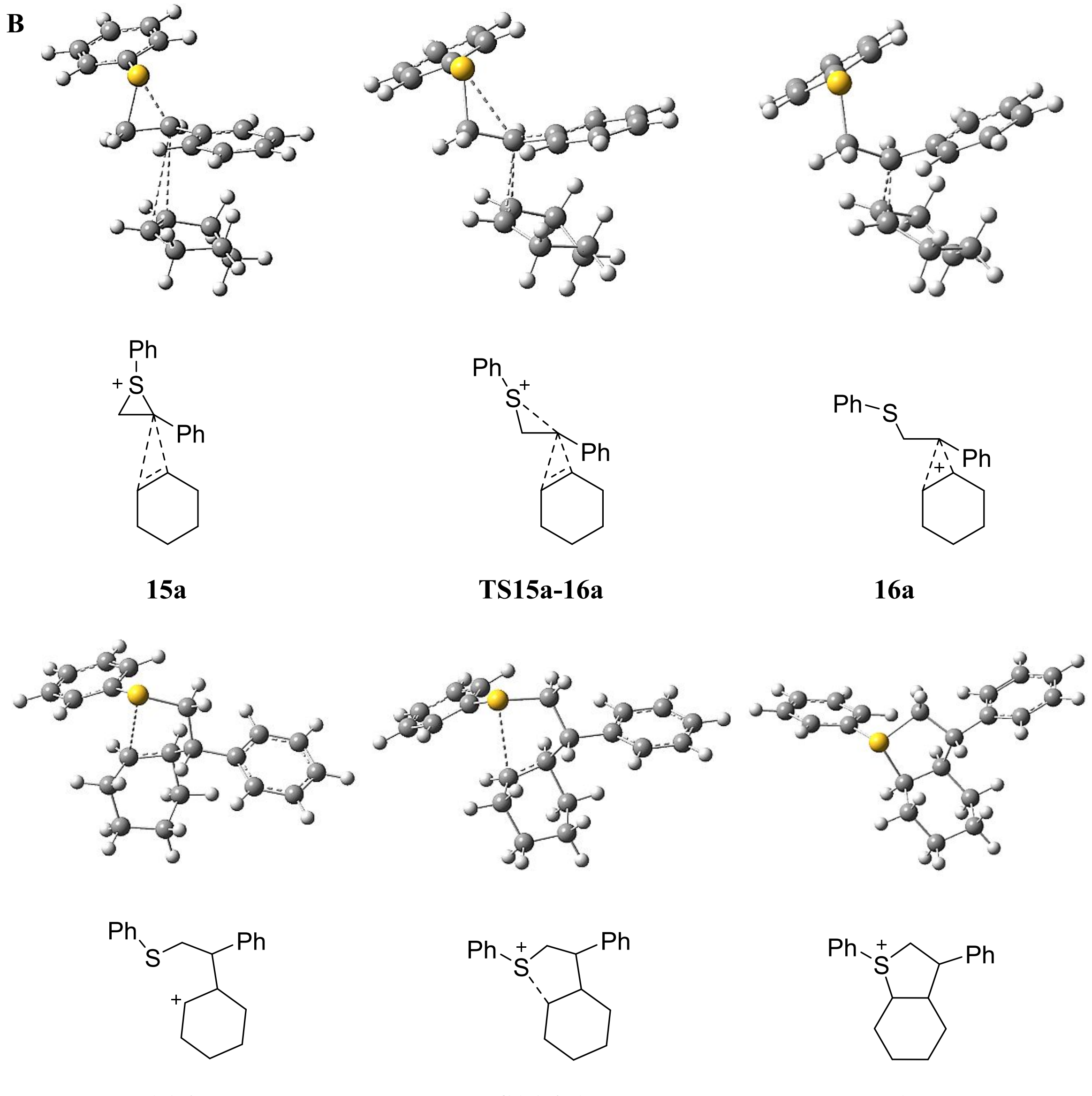

15a **TS15a-16a** **16a**

16a’ **TS16a’-17a** **17a**

Figure 5. A) Relative energy diagram for addition of cyclohexene (a: n = 1, black) and *cis*-cyclooctene (b: n = 3, red) to thiiranium ion **11** followed by ring closure to give **17a** and **17b** respectively. Energies given as ΔH (ΔG) in kJ mol^{-1} at M06-2X/def2-TZVP level of theory relative to the combined total of the free reactant energies. **B)** Gaussview optimised structures of key species **16a’**, **TS16’-17a** and **17a** with accompanying Chemdraw diagrams. (Refer to Supporting Information for *cis*-cyclooctene Gaussview structures).

The most plausible structure for the addition product formed was the bicyclic sulfonium ion **17**, analogous to Radom’s insertion product in **Figure 1**. DFT calculations were thus performed on the addition of both cycloalkenes to thiiranium ion **11** to further explore the mechanism. Following an exothermic ring opening by cyclohexene (**TS15a-16a**, ΔH‡ = -1.4 kJ mol^{-1}) at the benzylic carbon of thiiranium ion **11** (the alternative attack at the methylene carbon by cyclohexene gave ΔH‡ = +22.8 kJ mol^{-1}, see Supporting Information p S39 and is not predicted to occur), the addition product **17a** could be reached *via* the cyclopropylium ion **16a** ($\Delta H = +0.5$ kJ mol^{-1}) with this pathway viable within the margin of error of the theoretical method (**Figure 5**).[44] The small amount of product **17a** formed under the experimental conditions is also reflective of the large $\Delta G^{\ddagger}$ of +51.1 kJ mol^{-1} at the RDS (**TS12a-13a**, **Figure 5**), even with a large thermodynamic drive towards formation of -176 kJ mol^{-1}. The lower energy pathway for addition of *cis*-cyclooctene to **11**, particularly at the C-C bond formation step (**TS12b-13b**, $\Delta H^{\ddagger} = -12.3$ kJ mol^{-1}) and subsequent cyclopropylium ion **16b** ($\Delta H = -23.5$ kJ mol^{-1}), is due to reduced steric interactions between the cycloalkyl and benzyl moieties (Supporting Information p S45), and greater strain release of the larger cycloalkene.[45] The subsequent intermediate and ring closure transition state were not stable minima at the M06-2X/def2-TZVP level of theory for *cis*-cyclooctene, perhaps reflecting rapid capture of the secondary carbocation by the sulphur lone-pair. Overall, the lower energy RDS predicts a faster rate of reaction for *cis*-cyclooctene and this is reflected in the larger amount of product for the same reaction time compared to cyclohexene (**Figure 3**). The pathway is also much lower in energy compared to Radom's concerted mechanism (barrier of +393 kJ mol^{-1}) as it is step-wise and able to proceed through a discrete secondary carbocation **16'** (compare **Figures 1** and **5**).

Addition by the cycloalkene to a benzylic stabilised carbocation, where the thiiranium ion has undergone ring opening, was also considered due to strong evidence of this equilibria in solution.[46] However, not only was the required open structure found not to be a minima at the M06-2X/def2-TZVP level of theory in the gas-phase, but the $\Delta H^{\ddagger}$ of a transition state located for the addition of cyclohexene to the benzylic carbocation was found to be +26.1 kJ mol^{-1} relative to the free reactants (refer to Supporting Information p S41). As explained above, the fact that bimolecular IMR with endothermic barriers will not proceed in the gas-phase, combined with the lower energy pathway calculated for ring opening of the thiiranium ion, excludes addition by the cycloalkene to an 'open' benzylic carbocation.

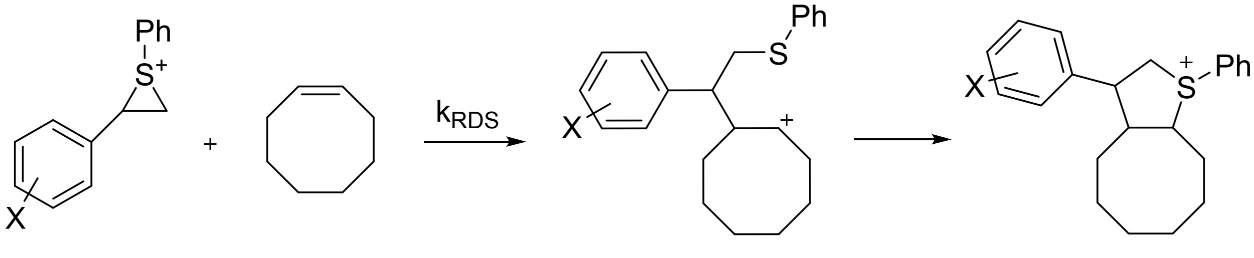

Scheme 5. Addition of *cis*-cyclooctene to thiiranium ions with electronic substituents to give bicyclic addition products *via* a secondary carbocation intermediate.

Now that the main reaction pathway for thiiranium ions with cycloalkenes had been established in the parent system **11**, we decided to explore electronic effects affecting the observed outcomes and reactivity. We proposed that by varying the electronic demand at the benzylic carbon, the position proposed to be involved in the rate-determining step for the addition pathway, the thiiranium ion electrophilicity could be modulated and the resulting rate of reaction with neutral cycloalkene varied.

Table 1. Pseudo 1st order reaction rates for ion-molecule reactions of thiiranium ions with varying electronic substituents and *cis*-cyclooctene (conc. *ca* 10^{11} molecules cm^{-3})*

	X	**σ** [47]	**σ^+**	**$k_{observed}$* (s^{-1})**	**$k_{absolute}$ (cm^3 $molecules^{-1}$ s^{-1})#**	**$k_{relative}$ (k_X/k_H)**
18	*m*-NO_2	0.710	0.674	2.8×10^{-1}	$(4.6 \pm 1.2) \times 10^{-12}$	13.9
19	*m*-OMe	0.115	0.047	2.4×10^{-2}	$(4.0 \pm 1.0) \times 10^{-13}$	1.21
11	H	0	0	2.1×10^{-2}	$(3.3 \pm 0.8) \times 10^{-13}$	1.00
20	*p*-CH_3	-0.170	-0.311	1.3×10^{-2}	$(2.1 \pm 0.5) \times 10^{-13}$	0.64
21	*p*-OMe	-0.268	-0.778	4.6×10^{-3}	$(7.5 \pm 1.9) \times 10^{-14}$	0.23

*determined by monitoring decrease in parent ion intensity #errors given as a conservative ± 25% of $k_{absolute}$[48]

A variety of sulphur substrates were prepared from the appropriate substituted styrenes by established methods (see experimental section). Thiiranium ions **18-21**, generated directly under ESI conditions from acetate precursors **33-36** and characterised by HRMS (see Supporting Information p S3-5), were isolated in the quadrupole ion-trap and then exposed to *cis*-cyclooctene (**Scheme 5**). The rates of consumption of the thiiranium ions were determined under pseudo first order conditions and the results summarised in **Table 1**. There is an increase in reactivity with increasing electron-withdrawing character of the substituent X as determined by the Hammett substituent constant, reflecting the increase in electrophilicity of the benzylic carbon. The plot of $\log(k_{rel}/k_H)$ *vs* σ gives a Hammett ρ constant of +1.69 ($R^2 = 0.974$), whilst $\log(k_{rel}/k_H)$ *vs* σ^+ gives a ρ constant of +1.20 with a lower R^2 of 0.947 (see Supporting Information p S11 for plots), noting the large ρ values are reasonable given the lack of solvent dampening.[49] The reduced correlation moving from σ to σ^+ values suggests that through-conjugation by the electron-donating substituents is not dominant in stabilising the positive charge on the benzylic carbon compared to the sulphur lone pair. More insight into the resonance demand of this system could be obtained by analysis with the Yukawa-Tsuno equation, but this requires a much a larger scope of substituents than presented here.[50] In all cases, there was no evidence for the formation of associative π-ligand exchange products.

Though the lack of exchange product observed for the above thiiranium ions was rationalised with the aid of calculations (**Figure 4**), the possibility of the observed addition reactivity being due to the isomeric sulphonium ions potentially formed *via* isomerisation during ESI has not been addressed. The assumption of similarities with the seleniranium ions in terms of structure may not be valid with suggestions of rapid isomerisation for oxiranium ions to oxonium ions in the gas-phase by Renzi *et al.* of concern, and so DFT calculations were performed to determine the barriers to formation of the potential sulphonium ions.[51]

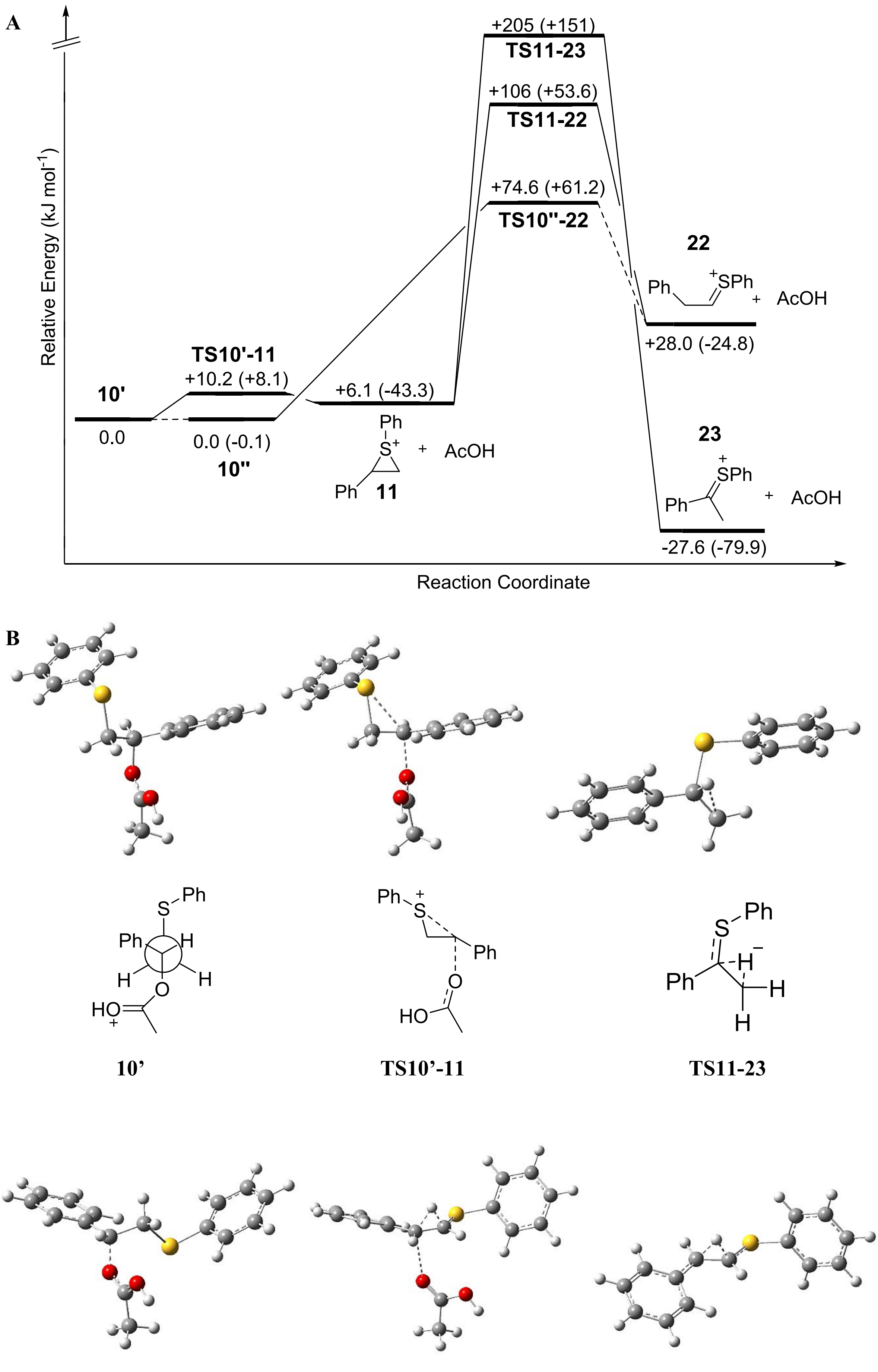
A
Relative Energy (kJ mol^{-1})
Reaction Coordinate
10'
0.0
TS10'-11
+10.2 (+8.1)
0.0 (-0.1)
10''
+6.1 (-43.3)
Ph
S+
Ph
11
+ AcOH
+205 (+151)
TS11-23
+106 (+53.6)
TS11-22
+74.6 (+61.2)
TS10''-22
22
Ph
+SPh
+ AcOH
+28.0 (-24.8)
23
+SPh
Ph
+ AcOH
-27.6 (-79.9)
B
S
Ph
Ph
H
H
H
O
HO
+
10'
Ph
+
S
Ph
O
HO
TS10'-11
S
Ph
H
−
Ph
H
H
TS11-23

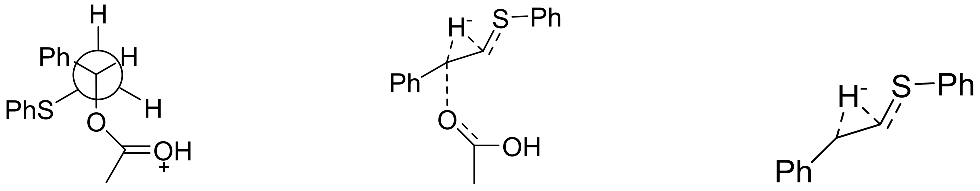

10'' **TS10''-22** **TS11-22**

Figure 6. A) Relative energy diagram of potential isomerisation pathways from protonated β-sulphur acetate **10'** to thiiranium ion **11** and sulphonium ions **22** and **23**. Energies given as ΔH (ΔG) in kJ mol^{-1} calculated at M06-2X/def2-TZVP relative to the protonated ion **10'**. Only key transition states and minima are shown, refer to Supporting Information p S12 for full pathways. **B)** Gaussview optimised structures of key species **10'**, **TS10'-11**, **TS11-23**, **10''**, **TS10''-22**, and **TS11-22** with accompanying Chemdraw diagrams.

Thus, we considered pathways for the isomerisation of the precursor **10** to sulphonium ions **22** and **23** (**Figure 6**). There are likely many conformers accessible for the protonated acetate precursor, but a manual coordinate search from the transition states identified the relevant minima **10'** and **10''** (refer to Supporting Information p S59-S60 for other conformers located). The low barrier of +10 kJ mol^{-1} for formation of thiiranium ion **11** from **10'** reflects the lack of observation of the protonated acetate precursor with the energy from ESI sufficient to induce departure of the leaving group (**Figure 6**). This is likely assisted by a large entropic driving force contributing to a Gibbs free energy change of -43 kJ mol^{-1} for thiiranium ion formation with accompanying vacuum removal of acetic acid. The calculations suggest similarly high barriers to isomerisation for sulphur as compared to the previous selenium work with the change in leaving group to an acetate having minimal impact on these trends.[36] Indeed, potential hydride migration pathways leading to formation of sulphonium ions **22** and **23** involve barriers >70 kJ mol^{-1} with those from the thiiranium ion itself +106 kJ mol^{-1} and +205 kJ mol^{-1} respectively (**Figure 6**). However, a consequence of the lower energy pathway from acetate precursors to thiiranium ion **11** is formation of **22** or **23** potentially occurring in the presence of solvent during the ESI process. This could allow for neutral solvent molecules to assist *via* mechanisms such as proton transport catalysis to allow for more isomerisation than expected based on the calculations on the isolated molecule.[52] This would particularly impact on the lowest hydride transfer barrier of +74.6 kJ mol^{-1} which produces the more reactive sulphonium ion **22** (**TS10''-22**, **Figure 6**).

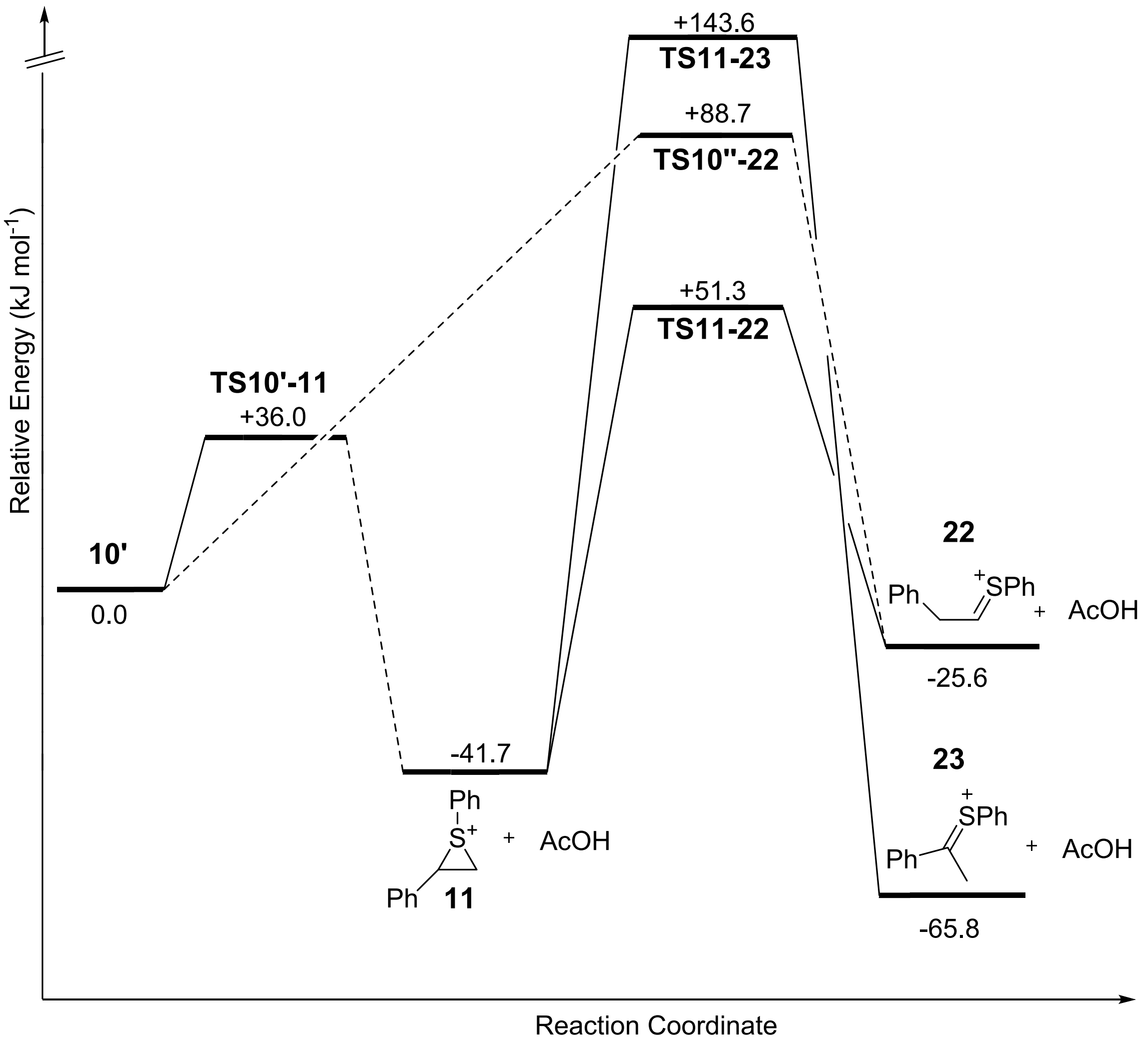

Figure 7. Relative energy diagram of potential isomerisation pathways from protonated β-sulphur acetate **10'** to thiiranium ion **11** and sulphonium ions **22** and **23** modelled in solution-phase with the polarizable continuum model (PCM). Energies given as ΔG in kJ mol^{-1} calculated at M06-2X/def2-TZVP relative to the protonated ion **10'**.

These barriers are, however, calculated in the gas-phase and given that the formation of thiiranium ion **11** occurs in the ESI source, the same potential isomerisation pathways were recalculated using the polarizable continuum model (PCM) (**Figure 7**).[53] Examination of the Gibbs free energy differences (not the enthalpic changes as explained) using this explicit solvent model suggests the same implications are present as with the gas-phase, even with the change in pathway topography. Despite a slightly higher barrier of +36.0 kJ mol^{-1} to form thiiranium ion **11**, the ion itself is in a lower energy well at -41.7 kJ mol^{-1} relative to the starting protonated acetate than compared with the gas-phase modelling in Figure 6. Hence, though one of the isomerisation barriers, **TS11-22**, is significantly lower compared to **10'**, the barrier relative to **11** is +93 kJ mol^{-1} (**Figure 7**). Overall, the formation of thiiranium ion **11** is still the lowest energy pathway with high Gibbs free energy barriers in solution-phase and high enthalpic barriers in the gas-phase to isomerisation.

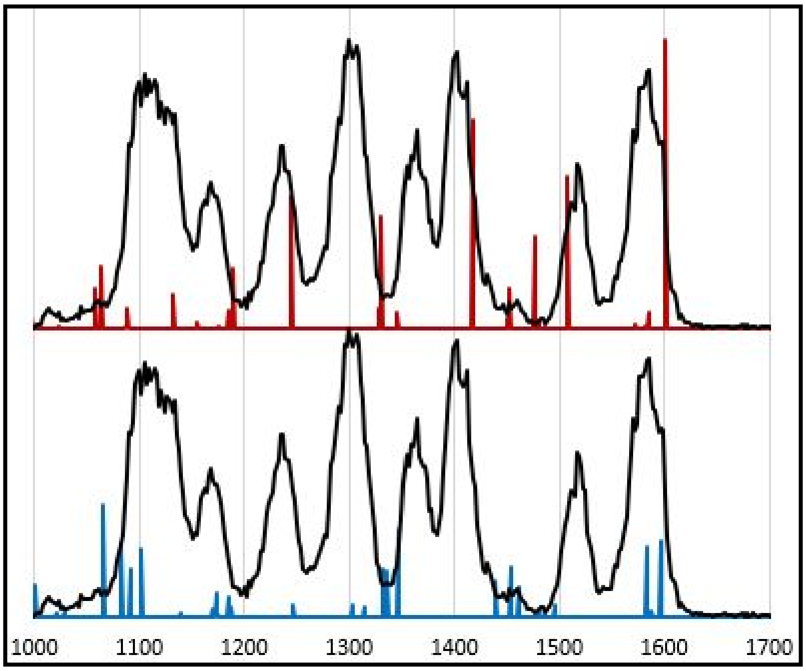

Figure 8. Infrared spectra of the *m/z* 213 ions. Experimental IRMPD spectra (black) in the 1000-1800 cm^{-1} range recorded at full laser power generated from ESI of **9**, compared to the theoretical IR spectrum of **a)** thiiranium ion **11** (red stick spectrum) and **b)** sulphonium ion **22** (blue stick spectrum) calculated at the B3LYP/6-311++G(d,p) level of theory with a scaling factor of 0.98 applied to the calculated frequencies.[54] In order to facilitate the comparison, calculated vibrational bands were convoluted by a Gaussian profile with a 20 cm^{-1} full width at half maximum. The maximum calculated intensities for the thiiranium and sulphonium ions are 172 and 92 km.mol^{-1} respectively.

To provide further evidence for the observed ion at *m/z* 213 indeed being that of **11**, infrared multiple photon dissociation (IRMPD) spectroscopy was conducted over a range of 1000-1800 cm^{-1}, similar to that previously performed with the selenium system.[36] Experimental IRMPD spectra of the *m/z* 213 ions and calculated IR absorption spectra of thiiranium ion **11** and sulphonium ion **22** are given in Figure 8. Eight bands can be distinguished in the experimental spectrum. Overall there is a better match with the thiiranium structure, and a tentative assignment is proposed in Table S1. Although the assignment of bands observed in the 1350-1450 cm^{-1} is not easy, there is a good quantitative agreement for five bands which can be considered as diagnostic. The relatively narrow bands observed at 1180, 1245, 1310, 1520 and 1585 cm^{-1} in particular match the absorption bands of thiiranium predicted at 1189, 1244, 1328, 1507, and 1601 cm^{-1} respectively (**Figure 8**).

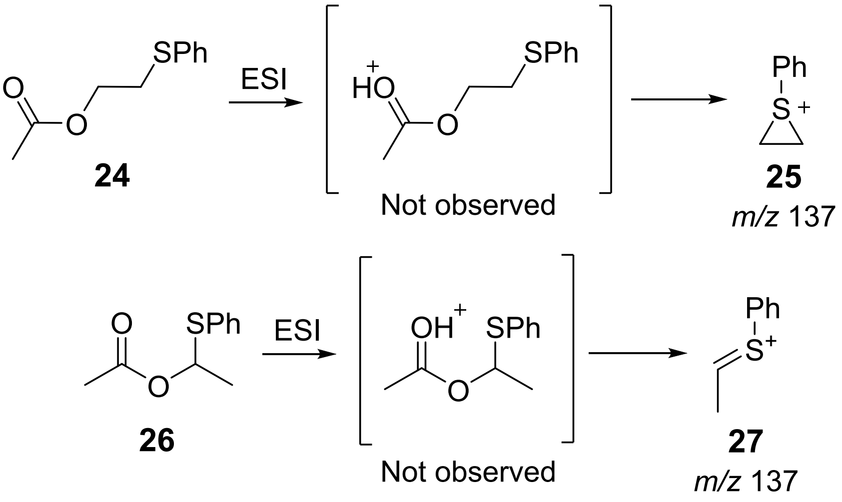

Scheme 6. ESI of acetate precursors **24** and **26** to give thiiranium ion **25** (*m/z* 137) and sulphonium ion **27** (*m/z* 137) respectively

Though this experimental and computational evidence was convincing, across both the sulphur and selenium systems studied thus far no chemical precursors to the -onium ions have been independently synthesised and tested for their resulting structure and reactivity with alkenes. To gain some insight into the relative reactivities of thiiranium and sulphonium ion intermediates with alkenes, two model precursors **24** and **26** were synthesised, which would feasibly give thiiranium ion **25** and sulphonium ion **27** respectively upon ESI (**Scheme 6**). Evidence for their formation was also attempted *via* IRMPD spectroscopy, but the photon dissociation yield was too low to yield good quality spectra. To support the assumption of the *trans*-sulphonium ion **27** being formed over the *cis* (as shown in Scheme 6), DFT calculations were performed on the acetate precursor and the ions themselves. Though the *cis* species was calculated to be only 3 kJ mol^{-1} less stable than the *trans*, only two conformers of the starting acetate precursor were located and both of these would lead to the *trans* sulphonium ion upon ESI (*cis*-precursor was found not to be a minimum at the M06-2X/def2-TZVP level of theory. See Supporting Information p S84-S87 for these structures). Hence, it is reasonable to assume in further analysis that it is the *trans* isomer that is dominant in the sulphonium ion mixture.

What has not been tested thus far was the experimental outcome of an IMR between a sulphonium ion and a neutral alkene in the gas-phase. However, this could now be investigated and compared between thiiranium ion **25** and the independently formed sulphonium ion **27**, with HRMS of the two ions supporting their formation (Supporting Information p S5-6). Both were introduced under ESI conditions as described previously and exposed to *cis*-cyclooctene with the results summarised in **Table 2**.

Table 2. Rates of IMR between *cis*-cyclooctene and thiiranium ion **25** or sulphonium ion **27**

***m/z* 137 Ion**	$k_{observed}$* (s^{-1})	$k_{absolute}$ (cm^3 molecules^{-1} s^{-1})	$k_{relative}$
Thiiranium	2.3×10^{-3}	$(3.7 \pm 0.9) \times 10^{-14}$	1
Sulphonium	6.0×10^{-1}	$(9.8 \pm 2.5) \times 10^{-12}$	265

*determined by monitoring decrease in the parent ion intensity

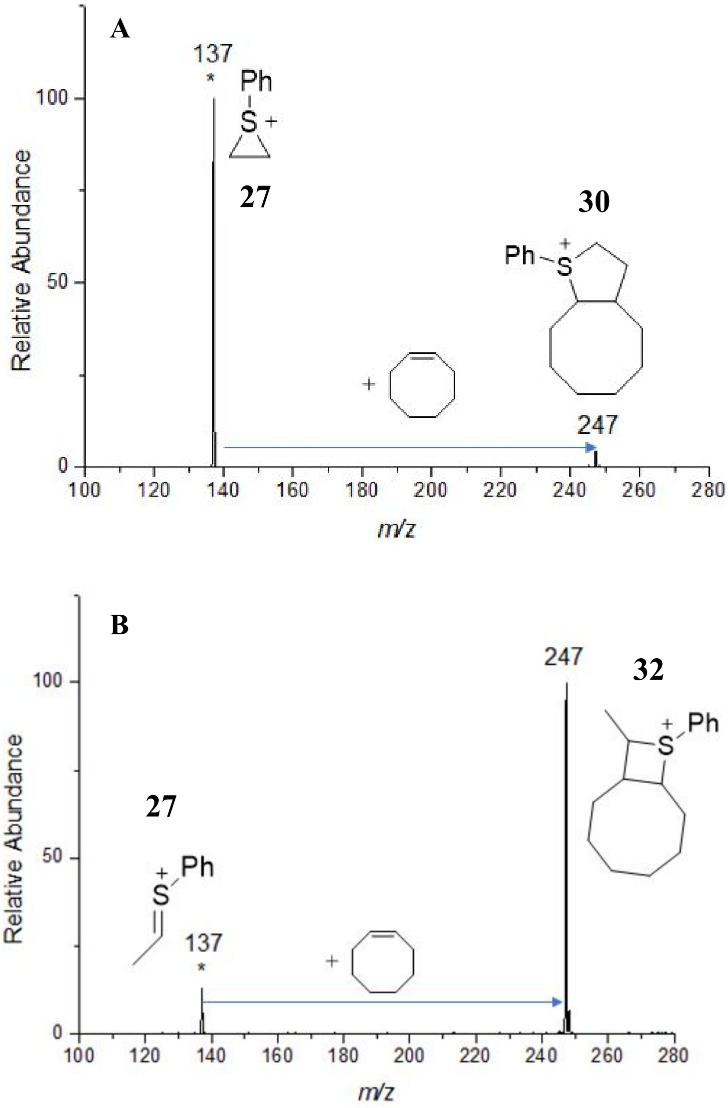

Figure 9. Ion-molecule reactions of *cis*-cyclooctene with **A)** thiiranium ion **25** *m/z* 137 (t = 4000 ms) and **B)** sulphonium ion **27** *m/z* 137 (t = 4000 ms). [*cis*-cyclooctene] *ca* 6 x 10^{10} molecules cm^{-3}.

The sulphonium ion **27** undergoes addition with *cis*-cyclooctene over 260 times fast than thiiranium ion **25** (**Table 2**). This is perhaps not surprising since, qualitatively, the weaker π-bond in the sulphonium ion is much easier to break than the σ-bond in the thiiranium ion. It is also possible, similar to **11**, that a small quantity of reactive sulphonium ion **27** is present from isomerisation of **25**, giving rise to the observed product following reaction with the cycloalkene (**Figure 9A**). However, any isomerisation would have to proceed over higher barriers than those calculated in Figure 6 as any stabilisation afforded by the benzyl system is absent. Indeed, Broer *et al.* have calculated the barrier for isomerisation of a similar small thiiranium ion (S-H instead of S-Ph) to the sulphonium ion to be +129 kJ.mol^{-1}.[55] Even if a small amount of sulphonium ion had formed in the ESI source, the kinetics obtained show that this species would rapidly be consumed and not be present in any significant amount after a few seconds of reaction time (**Table 2**, **Figure 9**). Given that the thiiranium ion **25** data was obtained from 1 to 15 second reaction time periods (refer to Supporting Information p S13 for the parent ion decay plot), this is the strongest evidence yet that it is indeed the thiiranium ion undergoing addition and not a sulphonium ion. To provide further support for this, DFT calculations were performed for addition of *cis*-cyclooctene to the two isomeric species (**Figure 10**).

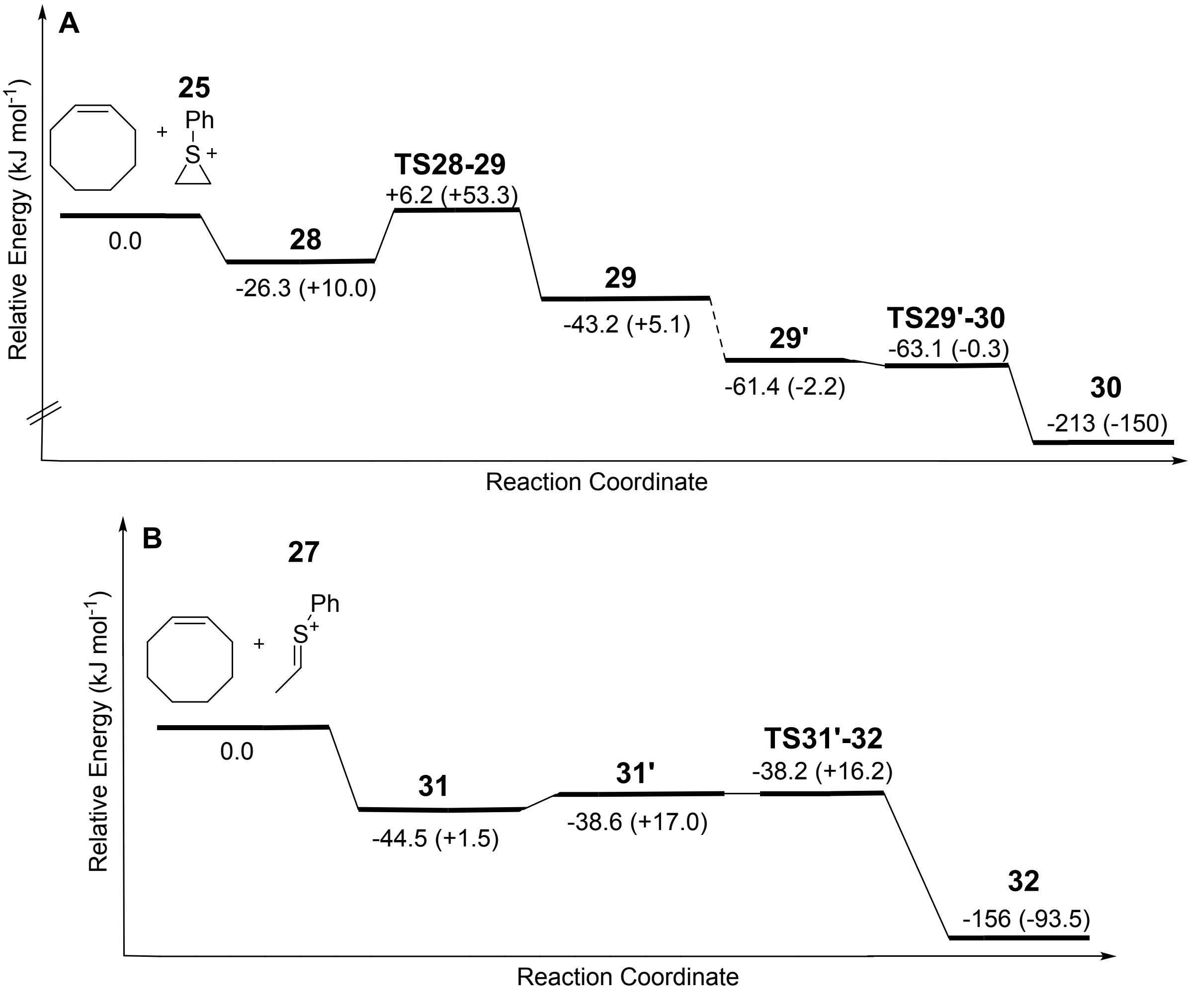

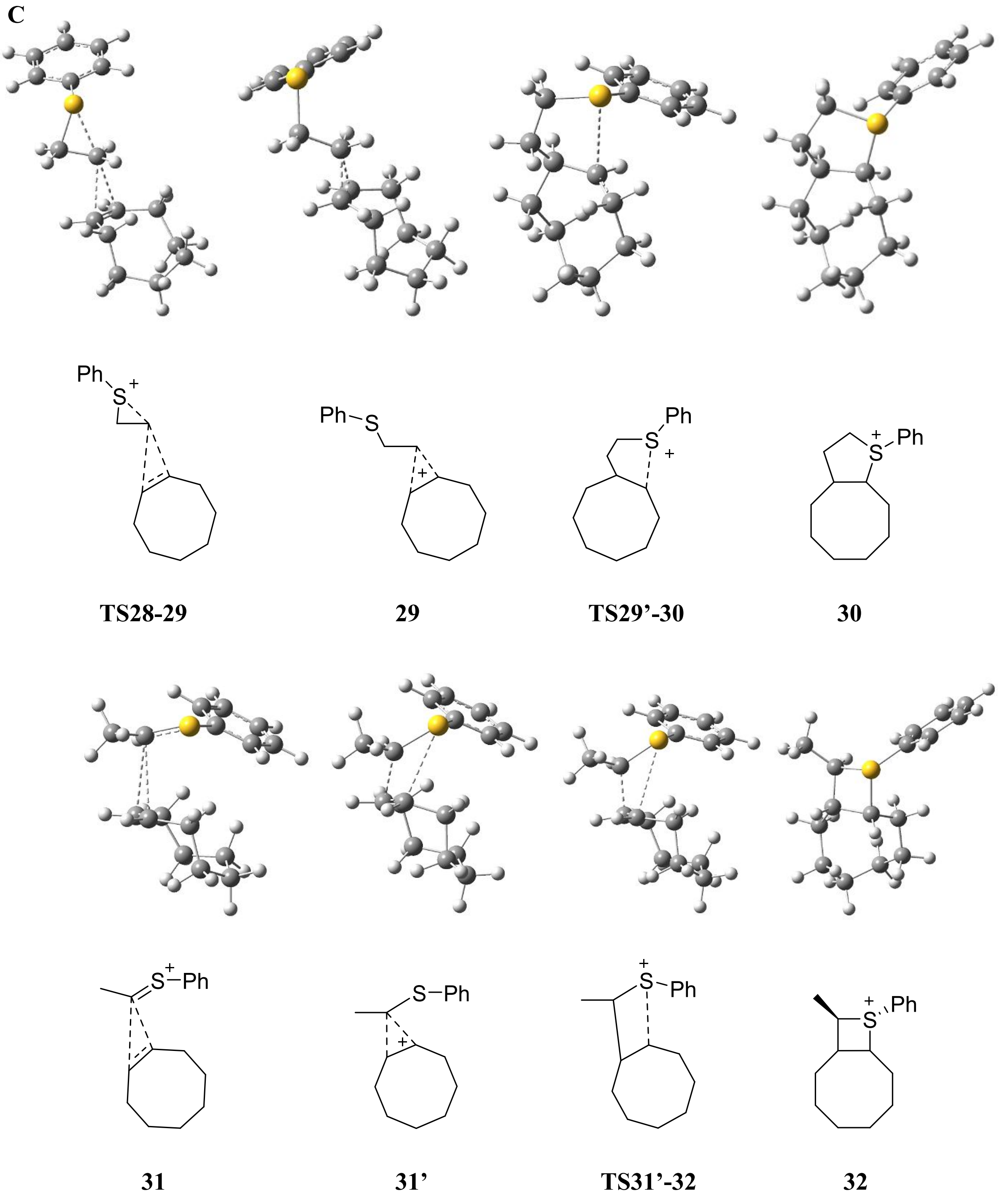

TS28-29 **29** **TS29’-30** **30**

31 **31’** **TS31’-32** **32**

Figure 10. Relative energy diagrams for addition of *cis*-cyclooctene to **A)** thiiranium ion **25** followed by ring closure to give **30** and **B)** sulphonium ion **27** followed by ring closure to give **32**. Energies given as ΔH (ΔG) in kJ mol^{-1} at M06-2X/def2-TZVP level of theory relative to the combined total of the free reactant energies. **C)** Gaussview optimised structures of key species **TS28-29**, **29**, **TS29’-30**, **30**, **31**, **31’**, **TS31’-32**, and **32** with accompanying Chemdraw diagrams.

Further examination of these pathways shows a relatively low barrier of +6.2 kJ mol^{-1} for *cis*-cyclooctene addition at thiiranium ion **25** (**Figure 10A**). Though slightly above the combined reactant energy, the small error in similar DFT methods of ± 5 kJ mol^{-1} for transition states and the fact that a

Boltzmann distribution of ions will be reacting means that it is still plausible for the reaction to proceed.[44] Indeed, the remainder of the pathway to addition product **30** is energetically favourable with little barrier for S-C bond formation (**TS29'-30**, **Figure 10A**). Taken together with a $\Delta G^{\ddagger}$ of +53.3 kJ mol^{-1} at the RDS, this explains why the rate of reaction of addition of *cis*-cyclooctene to thiiranium ion **25** is so slow at *ca* 10^{-14} cm^3 $molecules^{-1}$ s^{-1} (**Table 2**). Addition by the alkene to sulphonium ion **27** was found to be barrierless for the C-C bond forming step with a potential energy scan from the cyclopropylium ion **31'** proceeding smoothly to the separated reactants (see Supporting Information p S15). This is consistent with the much faster rate of reaction observed at *ca* 10^{-12} cm^3 $molecules^{-1}$ s^{-1} for addition to **27** as, once the initial complex is formed in the correct orientation, there is relatively barrierless pathway to form the *trans* addition product **32** (**Figure 10B**). Overall, comparison of addition of *cis*-cyclooctene to thiiranium ions **11** and **25**, and sulphonium ion **27** show good agreement between the experimental kinetic results (**Tables 1** and **2**) with the DFT theoretical barrier heights (or lack thereof) for C-C bond formation.

CONCLUSIONS

The findings contained in this paper have shown that thiiranium ions react with cyclic alkenes exclusively *via* an electrophilic addition pathway to give bicyclic products in the gas-phase. This is in contradiction with solution experiments that suggest direct transfer of the PhS^+ moiety between alkenes with DFT calculations suggesting high barriers for π-ligand exchange in the gas-phase. Further modelling showed the rate-determining step for addition to be the initial carbon-carbon bond forming step and this was supported with Hammett plots showing the rate of reactivity to increase as the benzylic position of thiiranium ion **11** became more electrophilic. The potential for sulphonium ion presence contributing to this addition pathway was examined through structural investigations with IRMPD spectroscopy and DFT calculations, which suggested the potential for a small amount of isomerisation. However, further studies on an independently isolated sulphonium ion suggested that due to its very fast reactivity with alkenes, calculated to be barrierless, only the thiiranium ion would be present at longer reaction times, supporting the fact that the latter exclusively undergoes electrophilic addition with alkenes in the gas-phase.

EXPERIMENTAL

Reagents: Cyclohexene (99%, Sigma Aldrich) and *cis*-cyclooctene (95%, Alfa Aesar) were used without further purification.

Nuclear Magnetic Resonance Spectroscopy: Proton and proton decoupled carbon NMR spectra for ^1H and ^{13}C nuclei respectively were recorded at ambient temperature (25 ºC) as solutions in the stated solvent using a Varian Inova 400 NMR spectrometer.

Synthetic Procedures: β-sulphenylacetate precursors **9** and **33-36** were synthesised in one step from diphenyldisulphide and the corresponding styrene derivative in the presence of diacetoxyiodobenzene and potassium iodide.[56] Most are known compounds and spectroscopic data matched those reported with the exception of the *m*-methoxyphenyl derivative (NMR spectra in Supporting Information p S16):

1-(3-Methoxyphenyl)-2-(phenylthio)ethyl acetate **34**: 94.8 mg, 62%, yellow oil.

^{1}H NMR ($CDCl_3$, 400 MHz) δ 7.40-7.38 (m, 2H), 7.31-7.21 (m, 4H), 6.93-6.83 (m, 3H), 5.87 (dd, J = 5.3, 8.0 Hz, 1H), 3.81 (s, 3H), 3.40 (dd, J = 8.2, 13.7 Hz, 1H), 3.24 (dd, J = 5.3, 13.9 Hz, 1H), 2.03 (s, 3H,). **^{13}C{^{1}H} NMR ($CDCl_3$, 100 MHz)** δ 170.0, 159.7, 140.6, 135.6, 130.1, 129.6, 129.0, 126.6, 118.9, 113.6, 112.4, 74.5, 55.3, 40.1, 21.0. **HRMS (ESI/OrbiTrap)** m/z [M – HOAc]$^+$ Calcd for $C_{15}H_{15}OS^+$ 243.0838; Found 243.0836.

The β-sulphenylacetate precursor **24** was obtained by acetylation of the corresponding hydroxyl derivative obtained from reaction of 2-bromoethanol and thiophenol under basic conditions.[57,58] The α-sulphenylacetate precursor **26** was synthesised *via* chlorination of ethyl phenyl sulphide with N-chorosuccinimide with subsequent displacement of the chloride by sodium acetate in DMF.[59,60]

Mass Spectrometry: Ion-molecule reactions (IMR) were performed by ionising the sample in a mixture of acetonitrile/formic acid (1% v/v) or a mixture of methanol/formic acid (1% v/v) *via* ESI into a Thermo Scientific linear ion trap quadrupole (LTQ) spectrometer, modified to allow introduction of a volatile neutral into the ion trap with the helium bath gas, as described previously.[61,62] It has been demonstrated that collisions with the helium bas gas quasi-thermalise the ions to room temperature under IMR conditions.[63] ESI solutions were introduced using a syringe pump operating at 5 μL.min^{-1} and by applying 4.0–4.8 kV to the ESI capillary relative to the heated capillary entrance to the mass spectrometer (250 °C). The sheath gas and lenses were tuned to optimize the signal of the ion, mass-selected for the most abundant isotopes of each element (^{1}H, ^{12}C, ^{14}N, ^{16}O, ^{32}S). High-resolution mass spectrometry (HRMS) characterisation of the generated thiiranium ions was conducted on a Thermo Scientific direct infusion NanoLC/OrbiTrap mass spectrometer and are available in the Supporting Information (p S3-6).

Quantum Chemistry Calculations: Standard density functional theory (DFT) calculations were performed using the Gaussian 16 revision *B.01* software package.[64] Optimized structures and energies were obtained with the M06-2X/def2-TZVP level of theory and incorporated zero-point vibrational energy corrections at 298 K.[65,66] The M06-2X method is applicable for main group thermochemistry and similar hybrid meta-GGA functionals (M05-2X) have been shown to accurately predict the structure of asymmetric oxiranium ions compared to the high-level couple-clustered CCSD method.[67] Vibrational frequency and intrinsic reaction-coordinate analyses were applied to confirm transition state structures (one imaginary frequency). Cartesian coordinates for all reported structures along with electronic, enthalpic and Gibbs free energies are provided in the Supporting Information (p S18-87).

IRMPD Spectroscopy: Infrared spectroscopic experiments were performed using an Esquire 3000+ quadrupole ion trap mass spectrometer (Bruker-Daltonics, Bremen, Germany) equipped with an ElectroSpray Ionization (ESI) source. As described in details elsewhere, a hole has been drilled in the ring electrode of the quadrupole ion trap allowing for the irradiation of mass-selected ions with an infrared beam.[68] Infrared activation is performed using the IR beam of the free electron laser (FEL) of the Centre Laser Infrarouge d'Orsay (CLIO).[69] IR FELs deliver highly intense IR pulses and have been shown to be particularly well suited for fragmenting all kind of molecular ions through an IR multiple photon dissociation (IRMPD) process.[54] The CLIO IR FEL delivers ~8 μs long macropulses of ~40 mJ at a 25 Hz repetition rate, which corresponds to a mean power of 1W. The bandwidth is ~0.5% of the central wavenumber. The IR FEL frequency is calibrated using a small fraction of the IR beam which passes through a polystyrene film. As a result, at each wavelength during the IR FEL scan, polystyrene absorption, and an MS^2 mass spectra are simultaneously recorded. Wavelength corrections can thus be made during the data treatment. IRMPD spectra of mass-selected ions were recorded in the 1000-1800 cm^{-1} range using the chromatogram mode of the ion trap instrument. Synchronization of the ion-trap and IR-FEL control programs allows for a stepwise (~5 cm^{-1}) change of the IR frequency at each step of the chromatogram. Each MS^2 mass spectrum is an average of 10 acquisitions. IRMPD spectra were acquired multiple times by varying the number of -3dB attenuators.

CONFLICT OF INTEREST STATEMENT

The authors declare that the research was conducted in the absence of any commercial or financial relationships that could be construed as a potential conflict of interest.

ACKNOWLEDGEMENTS

We thank the Australian Research Council for financial support for financial support (DP0770565 to JMW and DP180101187 to RAJO), the Australian Government for a Research Training Program (RTP) scholarship to S.B, and The University of Melbourne for the Melbourne Research Scholarship (MRS) to S.F.L. Financial support from the European Community's Horizon 2020 Programme CALIPSOplus (grant number 730872) is gratefully acknowledged. The HRMS spectra were acquired at the Mass Spectrometry and Proteomics Facility (MSPF), Bio21 Institute, The University of Melbourne. The DFT calculations were performed on the Spartan High Performance Computing (HPC) System hosted by Research Platform Services at the University of Melbourne.[70]

SUPPORTING INFORMATION

High-resolution mass spectra of all thiiranium ions. Mass spectra of all ion-molecule reactions and accompanying time-decay plots of the parent ion. Full isomerisation pathway expanded from Figure 6. Assignments of the vibrational modes for **11**. Potential energy scan for reaction of *cis*-cyclooctene with sulphonium ion **27**. ^{1}H-NMR and ^{13}C-NMR of *m*-methoxyphenyl derivative **34**. Gaussian cartesian coordinates and energies for all calculated species.

REFERENCES

---

[1] Smit, W.A.; Krimer, M.Z.; Vorob'eva, E.A. Generation and Chemical Reactions of Episulfonium Ions. *Tetrahedron Lett.* **1975**, *29*, 2451-2454.

[2] Schmid, G.H.; Macdonald, D.I. The Effect of Environment on the Reactions of Thiiranium Ions. *Tetrahedron Lett.* **1984**, *25*, 157-160.

[3] Modena, G.; Pasquato, L.; Lucchini, V. Thiiranium and Thiirenium Ions Chemistry and Stereochemistry. *Phosphorous, Sulfur, and Silicon.* **1994**, *95-96*, 265-282.

[4] Denmark, S.E.; Kornfilt, D.J.P. Catalytic, Enantioselective, Intramolecular Sulfenofunctionalization of Alkenes with Phenols. *J. Org. Chem.* **2017**, *82*, 3192-3222.

[5] Denmark, S.E.; Vogler, T. Synthesis and Reactivity of Enantiomerically Enriched Thiiranium Ions. *Chem. Eur. J.* **2009**, *15*, 11737-11745.

[6] Fox, D.J.; House, D.; Warren, S. Mechanisms of Sulfanyl (RS) Migrations: Synthesis of Heterocycles. *Angew. Chem. Int. Ed.* **2002**, *41*, 2462-2482.

[7] Gruttadauria, M.; Noto, R. Kinetic and Thermodynamic Control in the Cyclization *via* Thiiranium Ions. Stereoselective Synthesis of a 2,3,5,-Trisubstituted Tetrahydropyran Ring. *J. Heterocyclic Chem*., **2009**, *38*, 765-767.

[8] Hartmann, E.; Denmark, S.E. Structural, Mechanistic, Spectroscopic, and Preparative Studies on the Lewis Base Catalyzed, Enantioselective Sulfenofunctionalization of Alkenes. *Helv. Chim. Acta.* **2017**, *100*, e1700158.

[9] Grewal, G.; Kaila, N.; Franck, R.W. Arylbis(arylthio)sulfonium Salts as Reagents for the Synthesis of 2-Deoxy-*β*-glycosides. *J. Org. Chem.* **1992**, *57*, 2084-2092.

[10] Denmark, S.E.; Hartmann, E.; Kornfilt, D.J.P.; Wang, H. Mechanistic, Crystallographic, and Computational Studies on the Catalytic, Enantioselective Sulfenofunctionalization of Alkenes. *Nature Chem.* **2014**, *6*, 1056-1064.

[11] Matsumoto, K.; Kozuki, Y.; Ashikari, Y.; Suga, S.; Kushimura, S.; Yoshida, J.-I. Electrophilic Substitution Reactions Using an Electrogenerated $ArS(ArSSAr)^+$ Cation Pool as an ArS^+ Equivalent, *Tet. Lett.* **2012**, *53*, 1916-1919.

[12] Caggiano, L.; Davies, J.; Fox, D.J.; Moody, D.J.; Warren, S.; A Novel Silica Catalysed Stereoselective Cyclic Carbamate and Carbonate Rearrangement. *Chem. Commun.* **2003**, 1650-1651.

[13] Denmark, S.E.; Kornfilt, D.J.P.; Vogler, T. Catalytic Asymmetric Thiofunctionalization of Unactivated Alkenes. *J. Am. Chem. Soc.* **2011**, *133*, 15308-15311.

[14] Denmark, S.E.; Jaunet, A. Catalytic, Enantioselective, Intramolecular Carbosulfenylation of Olefins. *J. Am. Chem. Soc.* **2013**, *135*, 6419-6422.

---

[15] Denmark, S.E.; Chi, H.M. Catalytic, Enantioselective, Intramolecular Sulfenoamination of Alkenes with Anilines. *J. Org. Chem.* **2017**, *82*, 3826-3843.

[16] Tao, Z.; Robb, K.A.; Zhao, K.; Denmark, S. E. Enantioselective, Lewis Base-Catalyzed Sulfenocyclization of Polyenes. *J. Am. Chem. Soc.* **2018**, *140*, 3569-3573.

[17] Pasquato, L.; Herse, C.; Lacour, J. NMR Enantiodifferentiation of Thiiranium Cations by Chiral Hexacoordinated Phosphate Anions. *Tetrahedron Lett.* **2002**, *43*, 5517-5520.

[18] Capon, B.; McManus, S.P. *Neighbouring Group Participation*. Plenum Press: New York and London. **1976**, Vol. 1.

[19] Smit, W.A.; Zefirov, N.S.; Bodrikov, I.V.; Krimer, M. Z. Episulfonium Ions: Myth and Reality. *Acc. Chem. Res.* **1979**, *12*, 282-288.

[20] Gill, D.M.; Pegg, N.A.; Rayner, C.M. Nucleophilic Trapping of Thiiranium Ion Intermediates with Nitrogen Nucleophiles. *J. Chem. Soc. Perkin Trans. 1.* **1993**, 1371-1372.

[21] Schmid, G.; Strukelj, M.; Dalipi, S. The Products of the Reactions of Thiiranium Ions with Competing Nucleophiles. *Can. J. Chem.* **1987**, *65*, 1945-1950.

[22] Billings, S.B.; Woerpel, K.A. Nucleophilic Substitution Reactions of Sulfur-Substituted Cyclohexanone Acetals: An Analysis of the Factors Controlling Stereoselectivity. *J. Org. Chem.* **2006**, *71*, 5171-5178.

[23] Lucchini, V.; Modena, G.; Pasi, M.; Pasquato, L.; Different reactivity modes of cis and trans di-tert-butylthiiranium tetrafluoroborates with water. A new insight in the electrophilic additions to Z and E di-tert-butylethylenes. *J. Org. Chem.* **1997**, *62*, 7018-7020.

[24] Denmark, S.E.; Collins, W.R.; Cullen, M.D. Observation of Direct Sulfenium and Selenium Group Transfer from Thiiranium and Seleniranium Ions to Alkenes. *J. Am. Chem. Soc.* **2009**, *131*, 3490-3492.

[25] Solling, T.I.; Wild, S.B.; Radom, L. Are Pi-ligand Exchange Reactions of Thiirenium and Thiiranium Ions Feasible? An Ab Initio Investigation. *Chem. Eur. J.* **1999**, *5*, 509-514.

[26] Solling, T.I.; Radom, L. A G2 Study of SH^+ Exchange Reactions Involving Lone-Pair Donors and Unsaturated Hydrocarbons. *Chem. Eur. J.* **2001**, *7*, 1516-1524.

[27] Toshimitsu, A.; Nakano, K.; Mukai, T.; Tamao, K. Steric Protection of the Selenium Atom of the Episelenonium Ion Intermediate To Prevent both the Racemization of the Chiral Carbon and the Selenophilic Attack of the Carbon Nucleophiles. *J. Am. Chem. Soc.* **1996**, *118*, 2756-2757.

[28] Toshimitsu, A.; Tereda, M.; Tamao, K. Intramolecular Cyclization Reaction *via* a Sterically Protected Episelenonium Ion Intermediate. *Chem. Lett.* **1997**, 733-734.

[29] Toshimitsu, A.; Ito, M.; Uemura, S. The Stereochemistry of a Substitution Reaction *via* an Episelenonium Ion: Retention by a 2-Pyridylseleno Group *versus* Scrambling by a Phenylseleno Group. *J. Chem. Soc., Chem. Comm.* **1989**, 530-531.

---

[30] Okamoto, K.; Nishibayashi, Y.; Uemura, S.; Toshimitsu, A. Stereospecific Carbon-carbon Bond Formation by the Reaction of a Chiral Episelenonium Ion with Aromatic Compounds. *Tetrahedron Lett.* **2004**, *45*, 6137-6139.

[31] Denmark, S.E.; Kalyani, D.; Collins, W.R. Preparative and Mechanistic Studies Towards the Rational Development of Catalytic, Enantioselective Selenoetherification of Alkenes. *J. Am. Chem. Soc.* **2010**, *132*, 15752-15765.

[32] Gronert, S. Mass Spectrometric Studies of Organic Ion/Molecule Reactions. *Chem. Rev.* **2001**, *101*, 329-360.

[33] Gronert, S. Quadrupole Ion Trap Studies of Fundamental Organic Reactions. *Mass Spectrom. Rev.* **2005**, *24*, 100-120.

[34] O'Hair, R.A.J. The 3D Quadrupole Ion Trap Mass Spectrometer as a Complete Chemical Laboratory for Fundamental Gas-Phase Studies of Metal Mediated Chemistry. *Chem. Commun*. **2006**, 1469-1481.

[35] Osburn, S.; Ryzhov, V. Ion–Molecule Reactions: Analytical and Structural Tool. *Anal. Chem.* **2013**, *85*, 769-778.

[36] Lim, S.F.; Harris, B.L.; Khairallah, G.N.; Bieske, E.; Maitre, P.; da Silva, G.; Adamson, B.D.; Scholz, M.; Coughlan, N.J.A.; O'Hair, R.A.J.; Rathjen, M.; Stares, D.; White, J.M.; Seleniranium Ions Undergo π-ligand Exchange via an Associative Mechanism in the Gas Phase. *J. Org. Chem.* **2017**, *82*, 6289-6297.

[37] Bach, R.D. Ring Strain Energy in the Cyclooctyl System. The Effects of Strain Energy on [3+2] Cycloaddition Reactions with Azides. *J. Am. Chem. Soc.* **2009**, *131*, 5233-5243.

[38] Shea, K.J.; Kim, J. Influence of Strain on Chemical Reactivity. Relative Reactivity of Torsionally Strained Double Bonds in 1,3-Dipolar Cycloadditions. *J. Am. Chem. Soc.* **1992**, *114*, 4846-4855.

[39] Allinger, N.L.; Sprague, J.T. Conformational Analysis. LXXXIV. A Study of the Structures and Energies of Some Alkenes and Cycloalkenes by the Force Field Method. *J. Am. Chem. Soc.* **1972**, *94*, 5734-5747.

[40] Herges, R. Coarctate Transition States: The Discovery of a Reaction Principle. *J. Chem. Inf. Comput. Sci.* **1994**, *34*, 91-102.

[41] *m/z* 97 in Figure 3a) is an oxidation product of cyclohexene, observed previously.[36] *m/z* 293 in Figure 3a) is plausibly reaction of a diene impurity with thiiranium ion **11**. This was supported by reacting the ion with an authentic sample of 1,3-cyclohexadiene. See Supporting Information p S15.

[42] Ervin, K.M. Experimental Techniques in Gas-Phase Ion Thermochemistry. *Chem. Rev.* **2001**, *101*, 391-444.

[43] Dau, P.D.; Armentrout, P.B.; Michelini, M.C.; Gibson, J.K. Activation of Carbon Dioxide by a Terminal Uranium-Nitrogen Bond in the Gas-Phase: A Demonstration of the Principle of Microscopic Reversibility. *Phys. Chem. Chem. Phys.* **2016**, *18*, 7334-7340.

---

[44] Zheng, J.; Zhao, Y.; Truhlar, D.G. The DBH24/08 Database and Its Use to Assess Electronic Structure Model Chemistries for Chemical Reaction Barrier Heights. *J. Chem. Theory Comput.* **2009**, *5*, 808-821.

[45] Freeman, F.; Arledge, K.W. Chromyl Chloride Oxidations. VII. Kinetics and Mechanism of Electrophilic Addition to Cycloalkenes. *J. Org. Chem.* **1972**, *37*, 2656-2662.

[46] Pasquato, L.; Modena, G. The Complete and Irreversible Conversion of a *Cis* Carbon-Substituted Thiiranium Ion into the *Trans* Isomer. *Chem. Commun.* **1999**, 1469-1470.

[47] Leffler, J.E.; Grunwald, E. *Rates and Equilibria of Organic Reactions*. John Wiley and Sons, Inc.: New York. **1963**.

[48] Waters, T.; O'Hair, R. A. J.; Wedd, A. G. Catalytic Gas Phase Oxidation of Methanol to Formaldehyde. *J. Am. Chem. Soc.* **2003**, *125*, 3384-3396.

[49] Zeigler, B. E.; McMahon, T. B. Computational Analysis of Substituent Effects and Hammett Constants for the Ionization of Gas Phase Acids. *Comput. Theor. Chem.* **2013**, *1008*, 46-51.

[50] Reis, J.C.R.; Segurado, M.A.P.; Gomes de Oliveira, J.D. Improved Yukawa-Tsuno Equation and the Substituent Effect on Pyridine Basicity. *J. Phys. Org. Chem.* **1998**, *11*, 495-503.

[51] Renzi, G.; Roselli, G.; Grandinetti, F.; Filippi, A.; Speranza, M.; Eliminative Ring Opening of Oxiranium Ions in the Gas Phase. *Angew. Chem. Int. Ed.* **2000**, *39*, 1673-1676.

[52] Bohme, D.K. Proton Transport in the Catalysed Gas-Phase Isomerization of Protonated Molecules. *Int. J. Mass. Spectrom. Ion Process.* **1992**, *115*, 95-110.

[53] Tomasi, J.; Mennucci, B.; Cammi, R. Quantum Mechanical Continuum Solvation Models. *Chem. Rev.* **2005**, *105*, 2999-3094.

[54] MacAleese, L.; Maitre, P. Infrared Spectroscopy of Organometallic Ions in the Gas Phase: From Model to Real World Complexes. *Mass Spectrom. Rev.* **2007,** *26*, 583-605.

[55] Broer, W.J.; Weringa, W.D.; Nieuwpoort, W.C. Rearrangements and Fragmentations of $[C_2H_5S]^+$ Ions. *Org. Mass Spec.* **1979**, *14*, 543-549.

[56] Muangkaew, C.; Katrun, P.; Kanchanarugee, P.; Pohmakotr, M.; Reutrakul, V.; Soorukram, D.; Jaipetch, T.; Kuhakarn, C. $PhI(OAc)_2$/K1 Mediated 1,2-Acetoxysulfenylation of Alkenes: Facile Synthesis of β-Acetoxysulfides. *Tetrahedron*. **2013**, *69*, 8847-8856.

[57] Ranganathan, S.; Ranganathan, D.; Singh, S.K. A Practical and Convenient Synthesis of the Nitroethylene Transfer Reagent, 2-Nitroethyl Phenyl Sulfoxide. *Tetrahedron Lett.* **1987**, *28*, 2893-2894.

[58] Parham, W.E.; Motter, R.F. The Reaction of Vinyl Sulfides and Alkyl Sulfides with Butyllithium. *J. Am. Chem. Soc.* **1959**, *81*, 2146-2148.

[59] Avolio, S.; Malan, C.; Marek, I.; Knochel, P. Preparation and Reactions of Functionalized Magnesium Carbenoids. *Synlett*. **1999**, *11*, 1820-1822.

---

[60] Benneche, T.; Strande, P.; Wiggen, U. Synthesis of α-Haloalkyl Esters from α-Arylthioakyl Esters *Acta. Chemica. Scandinavica.* **1988**, *43*, 74-77.

[61] Donald, W.A.; McKenzie, C.J.; O'Hair, R.A.J. C-H Bond Activation of Methanol and Ethanol by a High-Spin Fe^{IV}O Biomimetic Complex. *Angew. Chem. Int. Ed.* **2011**, *50*, 8379-8383.

[62] Lam, A.K.Y.; Li, C.; Khairallah, G.; Kirk, B.B.; Blanksby, S.J.; Trevitt, A.J.; Wille, U.; O'Hair, R.A.J.; da Silva, G. Gas-Phase Reactions of Aryl Radicals with 2-Butyne: Experimental and Theoretical Investigation Employing the N-Methyl-pyridinium-4-yl Radical Cation. *Phys. Chem. Chem. Phys.* **2012**, *14*, 2417-2426.

[63] Donald, W.A.; Khairallah, G.N.; O'Hair, R.A.J. The Effective Temperature of Ions Stored in a Linear Quadrupole Ion Trap Mass Spectrometer. *J. Am. Soc. Mass Spectrom.* **2013**, *24*, 811-815.

[64] Frisch, M.J.; Trucks, G.W.; Schlegel, H.B.; *et al.* Gaussian, Inc., Wallingford CT, **2016**.

[65] Zhao, Y.; Truhlar, D.G. The M06 Suite of Density Functionals for Main Group Thermochemistry, Thermochemical Kinetics, Noncovalent Interactions, Excited States, and Transition Elements: Two New Functionals and Systematic Testing of Four M06-class Functionals and 12 Other Functionals. *Theor. Chem. Acc.,* **2008**, *120*, 215-241.

[66] Weigend, F.; Ahlrichs, R. Balanced Basis Sets of Split Valence, Triple Zeta Valence and Quadruple Zeta Valence Quality for H to Rn: Design and Assessment of Accuracy. *Phys. Chem. Chem. Phys.* **2005**, *7*, 3297-3305.

[67] Zhao, Y.; Truhlar, D.G. How Well Can New-Generation Density Functionals Describe Protonated Epoxides Where Older Functionals Fail? *J. Org. Chem.* **2007**, *72*, 295-298.

[68] Mac Aleese, L.; Simon, A.; McMahon, T. B.; *et al.* Mid-IR Spectroscopy of Protonated Leucine Methyl Ester Performed with an FTICR or a Paul Type Ion-trap. *Int. J. Mass Spectrom.* **2006,** *249*, 14-20.

[69] Prazeres, R.; Glotin, F.; Insa, C.; *et al.* Two-colour Operation of a Free-Electron Laser and Applications in the Mid-infrared. *Eur. Phys. J. D: Atomic, Molecular and Optical Physics*, **1998,** *3*, 87-93.

[70] Lafayette, L.; Sauter, G.; Vu, L.; Meade, B. Spartan Performance and Flexibility: An HPC-Cloud Chimera. OpenStack Summit, Barcelona, October 27, 2016.

For Table of Contents Only